Rare Metal Materials and Engineering
Volume 50, Issue 3, March 2021
Available online at www.rmme.ac.cn

Science Press

Cite this article as: Rare Metal Materials and Engineering, 2021, 50(3): 0829-0834.

ARTICLE

Material Characterization and Validation for Stress Relaxation of Ti-4Al-1.5Mn Alloy at High Temperature

Deng Tongsheng, Li Shang, Liang Yaqian, Sun Lu, Zhang Hantao

Faculty of Materials Metallurgy and Chemistry, Jiangxi University of Science and Technology, Ganzhou 341000, China

Abstract: The material characterization and validation of relaxation behavior of Ti-4Al-1.5Mn alloy at high temperature were investigated. Firstly, constitutive models for the relaxation behavior at 500, 600 and 700 °C were established based on the stress relaxation tests. Further, the models were applied to finite element software ABAQUS to simulate the influence of stress relaxation on the springback after V-bending. The results show that the stress relaxation is controlled by temperature and relaxation time. The relaxation process can be divided into two stages. In the first stage, the stress decreases fast. In the second stage, the stress decreases slowly. Finally, the residual stress decreases to a limit value, which is defined as relaxation limit. Both hyperbolic sine and time hardening model can predict the variation of stress relaxation. The predicted springback shows promising agreement with the corresponding experimental observations. Hyperbolic sine model is more reliable than the time hardening model. The study is of guiding significance for the design of precise forming process by means of relaxation process.

Key words: titanium alloy; stress relaxation; constitutive model; FEM; V-bending

Titanium alloys are widely used in aerospace applications due to their high strength-to-mass ratio, composite compatibility and excellent corrosion resistance[1-3]. However, they are difficult to form into complex components, especially at room temperature. Therefore, elevated temperature forming methods are developed, such as hot forming[4], hot stretch bending (HSB) [5], superplastic forming (SPF) [6-8], and hot incremental sheet forming (HISF)[9-11]. Springback reduction plays an extremely important role in some elevated temperature forming processes, such as hot sizing[12,13] and hot stretch bending[14]. The principle of springback reduction is leading a stress relaxation by maintaining the workpiece against the die for a selected dwell time with the controlled temperature. This allows the benefits of low residual stress and minimum springback[15,16].

Therefore, the material characterization for the stress relaxation behavior is the fundamental issue for these forming processes. Material characterization includes constitutive model, mechanical properties, microstructural evolution, etc. Zong et al[13,17] calculated the stress exponents of Ti-6Al-4V alloy at 650~800 °C. These obtained exponents reflect several mechanisms rather than one mechanism in the stress range. Xiao et al[18] described the stress relaxation behavior of Ti-6Al-4V sheet over the medium temperature range from 923 K to 1023 K and at several strain levels. Lee et al[19] conducted load relaxation tests (LRTs) on Ti-6Al-4V alloy at 700, 800, and 900 °C to determine the strain rate sensitivity and to establish constitutive behavior. Stress-strain rate plots obtained by LRT are in good agreement with the theoretical predictions based on the activation of grain-matrix deformation and particle/grain-boundary sliding (P/GBS). There are also several works about the other metallic materials. For example, Chen et al[20] proposed a modified model based on the Chaboche unified viscoplasticity theory to demonstrate the influence of prior loading strain rates on stress relaxation. Type 304 stainless steel and TIMETAL 21S were selected to verify the utility of the modified Chaboche model, and sat-

Received date: March 26, 2020
Foundation item: Natural Science Foundation of Jiangxi Province (20192BAB216005); Science and Technology Research Program of Jiangxi Educational Committee (GJJ170550)
Corresponding author: Deng Tongsheng, Ph. D., Lecturer, Faculty of Materials Metallurgy and Chemistry, Jiangxi University of Science and Technology, Ganzhou 341000, P. R. China, E-mail: dts115@jxust.edu.cn

isfactory results were obtained. This research focuses on the constitutive models. Mechanical properties were obtained from previous literatures. Meanwhile, the microstructure evolution were not discussed.

Most researches for the stress relaxation of titanium alloy focus on the Ti-6Al-4V alloy, which is the most widely used titanium alloy. Whereas, few reports discussed about the Ti-4Al-1.5Mn alloy. Ti-4Al-1.5Mn is used for frame structures in aircraft. The stress relaxation of this alloy is the key performance of those components. In the previous work, the authors carried out a set of stress relaxation tests on Ti-4Al-1.5Mn alloy at the temperature from 773 K to 973 K and characterized the relaxation behavior[21]. However, more constitutive models description and calibration are needed. This research focuses on the modelization and comparison of hyperbolic sine and time-hardening models to predict the relaxation behavior. The accuracy of two models was compared, and the Runge-Kutta algorithm with fourth-grade and fourth-order was employed to obtain the prediction curve of hyperbolic sine model. Moreover, the availability of these models in finite element (FE) software was validated by ABAQUS to predict the springback after V-bending experiments.

1 Experiment

The materials for stress relaxation tests were Ti-4Al-1.5Mn alloy. The chemical composition is listed in Table 1.

Specimens were prepared according to ASTM E328. The geometry of the specimen is shown in Fig.1.

The stress relaxation tests were carried out on the RWS-50 electronic creep testing machine. The strain was measured by three laser extensometers which were positioned on both sides of the specimen. Average value of the extensometers' data was considered as the actual strain. Testing temperature was 500, 600 and 700 °C respectively. Pre-tensile-strain was 4% and the relaxation is 2400 s. Moreover, the surface of the samples was coated with anti-oxidant. The stress-time curve was recorded during the tests.

A special device was designed and manufactured for the V-bending experiments, as show in Fig.2. The device was installed on GWTA105 electronic creep testing machine by bolts. The extensometer was placed on the special platform to measure the displacement. The specimen dimension was 30 mm×22 mm×1.5 mm. The bending angle was 90° and the fillets were 3 mm.

Table 1 Chemical composition of Ti-4Al-1.5Mn alloy (wt%)

Al	Mn	C	Fe	Si	Zr	O	N	H	Others	Ti
4.1	1.5	0.10	0.30	0.12	0.30	0.15	0.05	0.012	0.30	Bal.

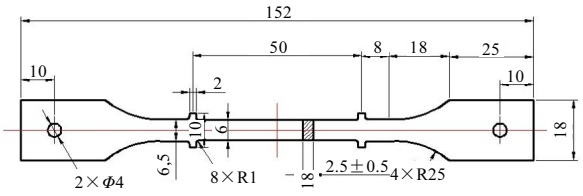

Fig.1 Schematic diagram of specimen for stress relaxation tests

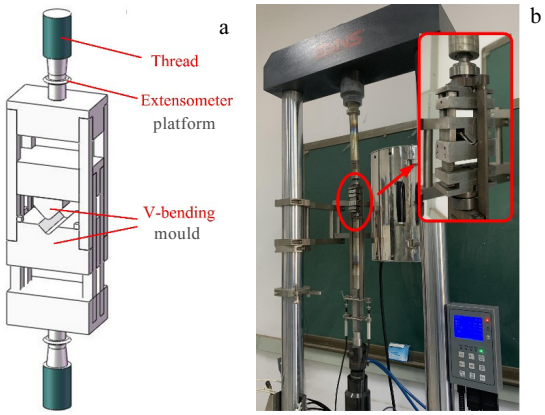

Fig.2 Setup for V-bending experiments: (a) design sketch and (b) setup on testing machine

The experimental temperature was set as 500 °C. According to theoretical calculation, the bending force was 5.88 kN. In order to ensure that the sheet can be bent to the designed state, drawing force of 5.9 kN was applied. After bending, the device kept the same deformation status for 0, 2, 5, 10, and 30 min respectively. Springback angle after unloading was measured to assess the effect of stress relaxation.

2 Constitutive Modeling

2.1 Hyperbolic sine model

In this research, cubic delay function was employed to fit the stress-time curve, as shown in Eq.(1):

$$\sigma = \sigma_0 + A_1 e^{-(t-t_0)/t_1} + A_2 e^{-(t-t_0)/t_2} + A_3 e^{-(t-t_0)/t_3} \quad (1)$$

Where σ is the instantaneous stress; σ_0 is the slack limit; t is relaxation time; A_1, A_2, A_3, t_0, t_1, t_2, and t_3 are parameters fitted by ORIGIN and listed in Table 2.

The comparison result between the fitted and experimental data is shown in Fig.3. The Adj. R-Square is 0.9996, 0.9994, 0.9991 for 500, 600 and 700 °C, respectively, which indicates that the fitting results are in good agreement with the experimental data.

The stress relaxation is mainly controlled by temperature and relaxation time. The relaxation curves can be divided into two stages. In the first stage, the stress decreases fast

with time. In the second stage, the stress decreases slowly. Finally, the residual stress decreases to a limit value, which is defined as the relaxation limit.

During the stress relaxation process, the following equation is obtained as follows:

$$\varepsilon_t = \varepsilon_e + \varepsilon_c \tag{2}$$

where ε_t is the total strain, ε_e is the elastic strain and ε_c is the creep strain induced by stress relaxation.

The total strain keeps invariant in the relaxation process, so the equation of strain rate relationship can be expressed as follows:

$$\dot{\varepsilon}_t = \dot{\varepsilon}_e + \dot{\varepsilon}_c = 0 \tag{3}$$

The creep strain rate can be obtained as follows:

$$\dot{\varepsilon}_c = -\dot{\varepsilon}_e = -\frac{\mathrm{d}\sigma}{E\,\mathrm{d}t} \tag{4}$$

where σ is stress and E is elastic modulus at the corresponding temperature.

Then $\dot{\varepsilon}_c$ can be calculated by differential computing of Eq.(1):

$$\dot{\varepsilon}_c = \frac{1}{E}\left(\frac{A_1}{t_1}\mathrm{e}^{-(t-t_0)/t_1} + \frac{A_2}{t_2}\mathrm{e}^{-(t-t_0)/t_2} + \frac{A_3}{t_3}\mathrm{e}^{-(t-t_0)/t_3}\right) \tag{5}$$

The relationship between creep strain rate and stress is shown in Fig.4.

The creep strain rate increases obviously with the increase of temperature, indicating that the temperature is one of the most important factors affecting the stress relaxation. As the stress decreases, the creep strain rate decreases rapidly and finally turns to zero, indicating that the stress is close to the relaxation limit.

The hyperbolic sine model is selected and expressed as follows[22,23]:

$$\dot{\varepsilon} = AF(\sigma)\exp\left(-\frac{Q}{RT}\right) \tag{6}$$

with

$$F(\sigma) = \begin{cases} \sigma^{n_1} & \alpha\sigma < 0.8 \\ \exp(\beta\sigma) & \alpha\sigma > 1.2 \\ [\sinh(\alpha\sigma)]^n & \text{for all } \sigma \end{cases} \tag{7}$$

where R is the universal gas constant; T is the absolute temperature; Q is the activation energy of hot deformation (kJ/mol); σ is the flow stress at a given strain; A, n_1, n, α and β are material constants with $\alpha=\beta/n_1$.

Take logarithm on both sides of hyperbolic sine equation under the condition of $\alpha\sigma<0.8$:

$$\ln\dot{\varepsilon} = \ln A_1 + n_1 \ln\sigma - \frac{Q}{RT} \tag{8}$$

Table 2 Fitting parameters value of cubic delay function

Temperature/°C	σ_0	t_0	A_1	t_1	A_2	t_2	A_3	t_3
500	166.41	−5.43	105.94	8.26	85.50	112.92	127.97	1021.52
600	32.79	−2.45	194.10	2.94	101.61	39.25	89.96	496.57
700	7.38	−3.33	87.80	19.26	319.51	1.65	31.49	380.98

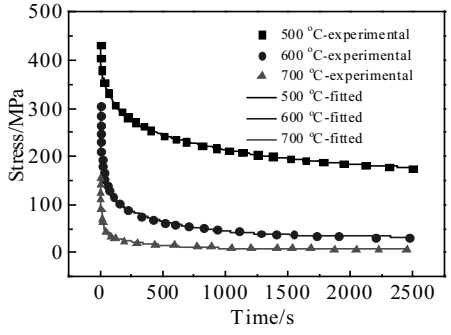

Fig.3 Comparison between the fitted and experimental data of stress relaxation

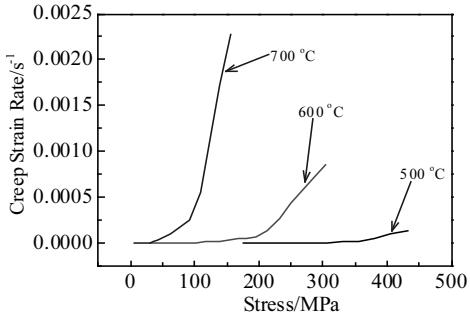

Fig.4 Relationship between creep strain rate and stress

n_1 can be obtained from the relationship between $\ln\dot{\varepsilon}$ and $\ln\sigma$, as shown in Fig.5.

Similarly, β can be obtained by taking logarithm on both sides of hyperbolic sine equation under the condition of $\alpha\sigma>1.2$. Then α is determined.

Take logarithm on both sides of hyperbolic sine equation under the condition for all σ:

$$\ln\dot{\varepsilon} = n\ln[\sinh(\alpha\sigma)] + B \tag{9}$$

with

$$B = \ln A_3 - \frac{Q}{RT} \tag{10}$$

n and B can be obtained from the relationship between $\ln\dot{\varepsilon}$ and $\ln[\sinh(\alpha\sigma)]$, as shown in Fig.6.

As shown in Eq.(10), B keeps a linear relationship with $1/T$. So the activation energy Q can be obtained easily. Finally, the parameter value of the hyperbolic sine model is listed in Table 3.

2.2 Time-hardening model

The creep strain can be conveniently modeled by the time hardening rule, which assumes that the creep strain rate has a power law relationship with the stress and time at a specific temperature. The relationship can be expressed as follows[24,25]:

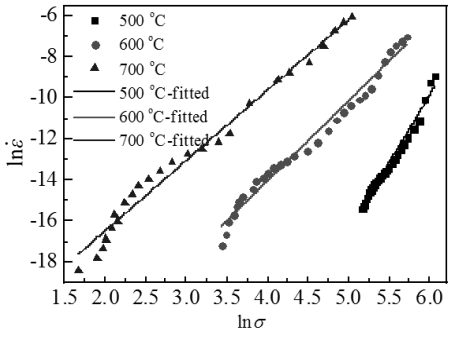

Fig.5 Relationship between $\ln\dot{\varepsilon}$ and $\ln\sigma$

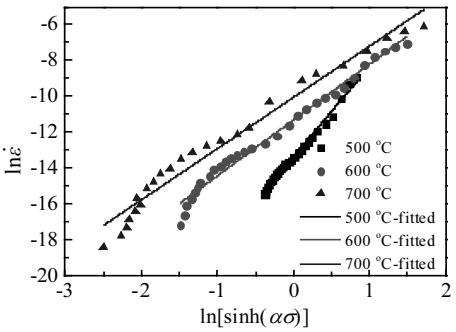

Fig.6 Relationship between $\ln\dot{\varepsilon}$ and $\ln[\sinh(\alpha\sigma)]$

Table 3 Parameters value of the hyperbolic sine model

Temperature/°C	A	α	n	Q/J·mol^{-1}
500		0.003 5	4.48	103 659
600	16.213	0.007 4	3.09	102 335
700		0.016 4	2.84	103 868

$$\dot{\varepsilon}_c = A\sigma^{n_t}t^m \tag{11}$$

where A is material parameter; n_t and m are the stress exponent and time hardening exponent, respectively.

The strain rate $\dot{\varepsilon}_c$ can be obtained by Eq.(5). Subroutine was programmed on the MATLAB software to calculate the parameters in the model at specific temperature. Finally, the parameters are listed in Table 4.

3 FE Simulation

The FE model for the stress relaxation was created by ABAQUS according to the V-bending experiments, as shown in Fig.7. The simulation is divided into three steps: bending, relaxation and springback, in which Dynamic/Explicit, Visco and Static/General were employed, respectively. The bending procedure is controlled by the displacement of the upper die. The period of relaxation procedure is defined according to the corresponding experiments. The period of springback is defined as 1. The materials properties were obtained from the previous work[21]. The mesh type of specimen is C3D8R with the length of 1 mm and width of 0.5 mm. Five Gauss integral points were used. The constitutive relationship of the stress relaxation is characterized by the hyperbolic sine or time-hardening model.

4 Results and Discussion

4.1 Accuracy of constitutive models

The functional relationship of $\sigma=f(t)$ is needed to confirm the accuracy of the constitutive models. For the hyperbolic sine model, the ordinary differential equation depends on Eq.(6) and can be expressed as follows:

$$\frac{\mathrm{d}\sigma}{\mathrm{d}t} = -EA[\sinh(\alpha\sigma)]^n \exp(-\frac{Q}{RT}) \tag{12}$$

The Runge-Kutta algorithm with fourth-grade and fourth-order is employed to solve the equation. The iterative equations can be expressed as follows:

$$\begin{cases} k_1 = -EA[\sinh(\alpha\sigma_i)]^n \exp(-Q/RT) \\ k_2 = -EA\{\sinh[\alpha(\sigma_i + 0.5hk_1)]\}^n \exp(-Q/RT) \\ k_3 = -EA\{\sinh[\alpha(\sigma_i + 0.5hk_2)]\}^n \exp(-Q/RT) \\ k_4 = -EA\{\sinh[\alpha(\sigma_i + hk_3)]\}^n \exp(-Q/RT) \\ \sigma_{i+1} = \sigma_i + \dfrac{h}{6}(k_1 + 2k_2 + 2k_3 + k_4) \end{cases} \tag{13}$$

The stability region for algorithm is $-2.78<h\lambda<0$. So λ stands for:

$$\lambda = \frac{\partial f}{\partial \sigma} = -EAn\alpha\left[\sinh(\alpha\sigma_n)\right]^{n-1} \exp(-\frac{Q}{RT})\cosh(\alpha\sigma_n) \tag{14}$$

In that case, the range of λ is (0, 45.15), (0, 2.225), and (0, 0.673) at 500, 600 and 700 °C, respectively. In the present work, λ is set as 0.1. The comparison between the experimental and predicted stress-time curves is shown in Fig.8.

Table 4 Parameters of the time-hardening model

Temperature/°C	A	n_t	m
500	2.06×10^{-12}	3.023	−0.495 6
600	1.03×10^{-10}	2.763	−0.334 2
700	3.06×10^{-9}	2.647	−0.222 4

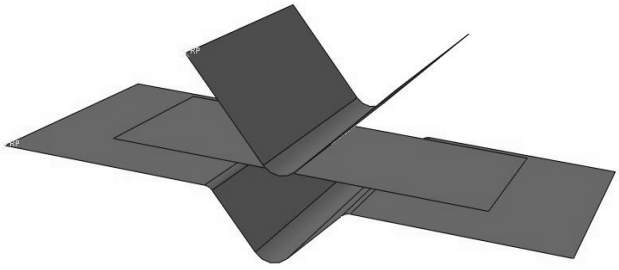

Fig.7 Finite element model of V-bending

As the time hardening equation is determined, the predicted stress can be obtained:

$$\sigma = (\frac{\dot{\varepsilon}}{A t^m})^{\frac{1}{n}} \quad (15)$$

The comparison between the experimental and time hardening model predicted stress-time curves is shown in Fig.9.

It can be seen that both hyperbolic sine and time hardening models predict the stress relaxation well, especially at the temperature of 500 and 600 °C.

4.2 Reliability of finite element prediction

The variation of stress in the specimen can be obtained in the visualization module through ABAQUS. Fig.10 shows the stress relaxation phenomenon at 500 °C for 30 min. The stress decreases in the relaxation stage according to the law of stress relaxation curves.

The springback is defined as the change of angle. In the FE code, the node coordinates before and after springback on the sheet are exported. The coordinates are plotted by AUTOCAD to measure the angle variation. The springback comparison between experimental data and FE prediction is shown in Fig.11.

It can be seen from the comparison that both hyperbolic sine and time hardening models are applicable to predict the stress relaxation and springback in ABAQUS. The springback data show that the FE simulation at 0 min is higher than the experimental datum. That is because in the experiment, unloading cannot be executed immediately, resulting in the stress relaxation after bending. Moreover, hyperbolic sine model is more reliable than the time hardening model. The reason may be attributed to the construction of hyperbolic sine model. The hyperbolic sine equation is developed from Garofalo and Arrhenius equation, which is more accurate to characterize the stress relaxation process.

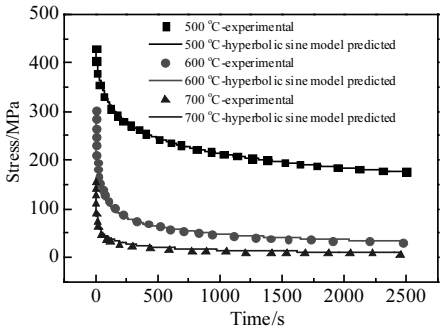

Fig.8 Comparison between experimental and hyperbolic sine model predicted stress-time curves

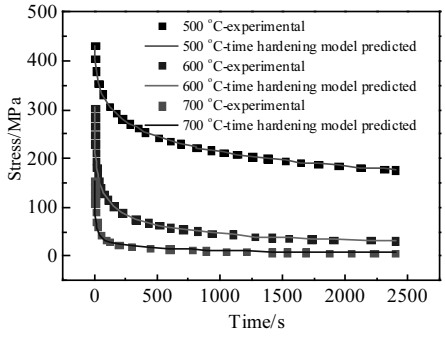

Fig.9 Comparison between experimental and time hardening model predicted stress-time curves

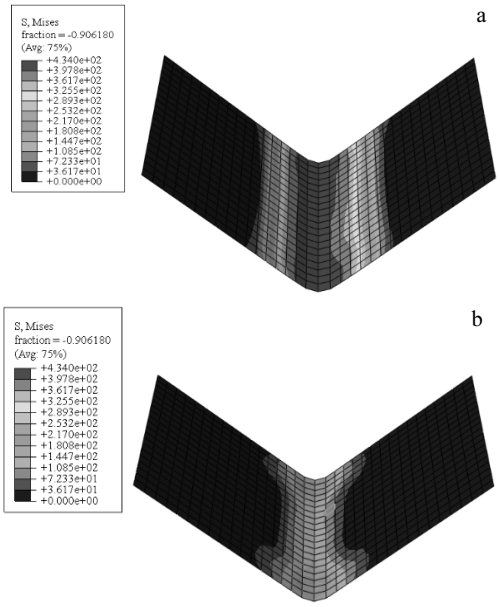

Fig.10 Mises stress of the specimen before (a) and after (b) relaxation

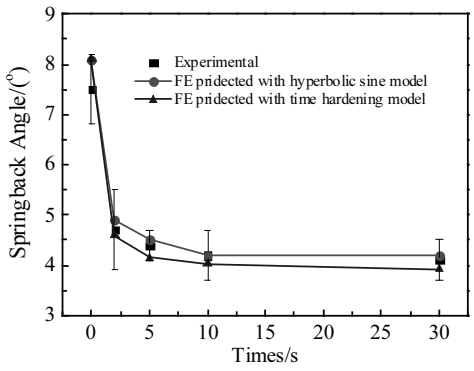

Fig.11 Comparison between experimental and FE predicted springback

5 Conclusions

1) The stress relaxation is controlled by temperature and relaxation time. The relaxation curves can be divided into two stages. In the first stage, the stress decreases fast with time. In the second stage, the stress decreases slowly. Finally, the residual stress decreases to a limit value, which is defined as the relaxation limit.

2) Both hyperbolic sine and time hardening models can well predict the relaxation behavior of Ti-4Al-1.5Mn alloy at high temperature.

3) The predicted springback in finite element model shows promising agreement with the corresponding experimental observations. Hyperbolic sine model is more reliable than the time hardening model.

References

1 Boyer R. *Materials Science and Engineering A*[J], 1996, 213 (1): 103

2 Zhang L C, Liu Y J, Li S J *et al. Advanced Engineering Materials*[J], 2018, 20 (5): 1700 842

3 Aghion E, Guinguis I, Goldman J. *Advanced Engineering Materials*[J], 2015, 17 (5): 626

4 Chen F K, Chiu K H. *Journal of Materials Processing Technology*[J], 2005, 170 (1): 181

5 Deng T S, LI D S, Li X Q. *Journal of Engineering Manufacture*[J], 2015, 230 (3): 506

6 Wang G C, Fu M W, Li J *et al*. *Advanced Engineering Materials*[J], 2014, 16 (1): 21

7 Brewer W D, Bird R K, Wallace T A. *Materials Science and Engineering A*[J], 1998, 243 (1): 299

8 Zhu X J, Tan M J, Zhou W. *Scripta Materialia*[J], 2005, 52 (7): 651

9 Ambrogio G, Filice L, Gagliardi F. *Materials & Design*[J], 2012, 34: 501

10 Fan G Q, Gao L, Hussain G *et al. International Journal of Machine Tools and Manufacture*[J], 2008, 48 (15): 1688

11 Ma L W, Mo J H. *Journal of Engineering Manufacture*[J], 2008, 222 (3): 373

12 Zhou Z F, Ni X H, Zhu X J. *Applied Mechanics & Materials*[J], 2014, 665: 21

13 Liu P, Zong Y Y, Shan D B *et al*. *Materials Science and Engineering A*[J], 2015, 638 (3): 106

14 Guo G Q, Li D S, Li X Q *et al*. *The International Journal of Advanced Manufacturing Technology*[J], 2017, 92 (5-8): 1707

15 Minakawa K, Keskar A R, Barb A. *US Patent*, 20070261463[P]. 2006

16 Polen L A, Houston T S, Owens J E. *US Patent*, 20100071430 [P]. 2009

17 Zong Y Y, Liu P, Guo B *et al. Materials Science and Engineering A*[J], 2015, 620(2): 172

18 Xiao J J, Li D S, Li X Q *et al*. *Rare Metal Materials and Engineering*[J], 2015, 44 (5): 1046

19 Lee T, Kim J H, Semiatin S *et al*. *Materials Science and Engineering A*[J], 2013, 562 (1): 180

20 Chen W F, Wang F H, Kitamura T *et al. International Journal of Mechanical Sciences*[J], 2017, 133: 883

21 Deng T S, Li D S, Li X Q *et al*. *Procedia Engineering*[J], 2014, 81: 1792

22 Mosleh A, Mikhaylovskaya A, Kotov A *et al*. *Metals*[J], 2017, 7 (12): 568

23 Lin Y C, Chen X M. *Materials & Design*[J], 2011, 32 (4): 1733

24 Fan Y N, Shi H J, Tokuda K. *Materials Science and Engineering A*[J], 2015, 625 (1): 205

25 Wang Y Q, Spindler M W, Truman C E *et al*. *Materials & Design*[J], 2016, 95: 656

Ti-4Al-1.5Mn 合金高温应力松弛本构模型及应用验证

邓同生，李 尚，梁雅倩，孙 露，张瀚韬

(江西理工大学 材料冶金化学学部，江西 赣州 341000)

摘 要：研究了 Ti-4Al-1.5Mn 合金在 500~700 ℃的应力松弛特性，首先在蠕变试验机上开展了该合金 500、600 和 700 ℃条件下的松弛试验，基于松弛数据分别建了双曲正弦和时间硬化两类本构模型，并对模型的预测精度进行了预测。随后把 2 类本构模型应用于 ABAQUS 软件对板材 V 形弯曲过程进行了仿真分析。结果表明，应力松弛的影响因素主要有温度和时间，松弛过程可以分为 2 个阶段，第 1 阶段应力快速下降，第 2 阶段缓慢下降并逐渐稳定于松弛极限。双曲正弦和时间硬化模型均可以对松弛过程进行较准确地预测，V 形弯曲后回弹结果表明双曲正弦比时间硬化模型具有更高的预测精度。研究结果对利用应力松弛进行精确成形的工艺设计具有指导意义。

关键词：钛合金；应力松弛；本构模型；有限元模拟；V形弯曲

作者简介：邓同生，男，1987 年生，博士，讲师，江西理工大学材料冶金化学学部，江西 赣州 341000，E-mail: dengtongsheng@jxust.edu.cn